Electro-engineered polymeric films for the development of sensitive aptasensors for prostate cancer marker detection

Pawan Jolly[1], Anna Miodek[1,‡,*], Deng-Kai Yang[2], Lin-Chi Chen[2], Matthew D. Lloyd[3], Pedro Estrela[1,*]

[1] Department of Electronic and Electrical Engineering, University of Bath, Claverton Down, Bath BA2 7AY, United Kingdom

[2] Department of Bio-Industrial Mechatronics Engineering, National Taiwan University, Taipei 10617, Taiwan

[3] Department of Pharmacy and Pharmacology, University of Bath, Claverton Down, Bath BA2 7AY, United Kingdom

[‡] Current address: Alternative Energies and Atomic Energy Commission (CEA), Institute of Biomedical Imaging (I²BM), Molecular Imaging Research Center (MIRCen), 18 route du Panorama, 92265 Fontenay-aux-Roses, France

KEYWORDS: AMACR (P504S); Amperometric; Aptamer; Aptasensor; Electrochemical; PEG; Polypyrrole; Prostate Cancer

Supporting Information Placeholder

ABSTRACT: We report the development of a simple surface chemistry strategy for the construction of sensitive aptasensors on a polypyrrole (PPy) – polyethylene glycol (PEG) platform in order to provide enhanced anti-fouling properties. We report the covalent modification of a PPy film formed on a gold electrode by PEG molecules, without prior chemical functionalization of the pyrrole monomer. This process was mediated by electro-oxidation of amine groups present on the one of the PEG's end chains. Poly-histidine modified aptamers were immobilized to this surface via a Nα,Nα-Bis(carboxymethyl)-L-lysine ANTA/Cu^{2+} redox complex covalently attached to the PPy-PEG adduct. The fabricated aptasensor was then utilized for the detection of α-methylacyl-CoA racemase (AMACR; P504S), an emerging biomarker for prostate cancer. Protein/aptamer interactions were monitored through variation of the copper redox signal, using the square wave voltammetry (SWV) technique. We demonstrate that the PPy-PEG-ANTA/Cu^{2+} hybrid material is characterized by enhanced anti-fouling properties and sensitivity. The aptasensor was able to detect AMACR down to 5 fM both in buffer and spiked human plasma with a limit of detection (LOD) of 0.15 fM and 1.4 fM, respectively. The developed aptasensor can be generalized for use with any type of aptamer-based sensor.

Prostate cancer (PCa) is a leading cause of cancer-related mortality among men worldwide.[1] Whilst prostate specific antigen (PSA) remains the benchmark for prostate cancer diagnosis, its use is considered unreliable due to lack of specificity. In particular, it is difficult to identify malignancy in patients with intermediate levels of PSA (4–10 ng/mL).[2] Early diagnosis of PCa is critical in defining treatment options, which can only be achieved by looking at panels of established and emerging biomarkers as well as novel detection techniques.[1,3] One of the potential biomarkers that has been gaining significant attention is α-methylacyl-CoA racemase (AMACR; P504S). AMACR is an isomerase involved in peroxisomal β-oxidation of branched-chain fatty acids. Recent studies have reported that AMACR is overexpressed in the majority of prostate malignancies as compared to normal and benign glands.[4] Most importantly, AMACR has been shown to have higher sensitivity and specificity than PSA for PCa identification in humoral immune assays, especially those with intermediate levels of PSA.[5] Although AMACR is a tissue biomarker[6], its presence in body fluids of PCa patients has also been reported.[2,7]

Recently, several research groups have tried to develop biosensors for AMACR detection.[8] In 2014, Yang *et al.*[9] first reported an anti-AMACR DNA aptamer (AMC51) with a dissociation constant of 44 nM and demonstrated a fluorescent enzyme-linked aptamer assay (ELAA) for AMACR detection, which featured a low detection limit of 0.44 nM. A DNA aptamer is a ligand binding single stranded DNA that binds to its target with high affinity and specificity by undergoing conformational changes.[10] Compared to antibodies, aptamers have several advantages including ease of synthesis and modification, chemical stability, small size, and low immunogenicity. These features make aptamers promising alternatives to antibodies for biosensor research.[3,11]

In this work, we present the development of an electrochemical AMACR aptasensor based on electro-patterned polyethylene glycol (PEG) on polypyrrole (PPy) film. PEG as a polymer has been widely used to develop biosensors, due to its anti-fouling properties.[12] However, it becomes difficult to employ PEG in an electrochemical platform due to its electri-

cal insulation properties. Nevertheless, several research groups have demonstrated the use of PEGs on electrochemical platforms. For example, Estrela *et al.*[13] developed an electrochemical biosensor for cyclin-dependent kinase protein detection using peptide aptamers and PEG, while Kjallman *et al.*[14] reported a DNA-based biosensor using PEG. Akhtar *et al.*[15] demonstrated a design of a PEG-aptamer for detection of ochratoxin A; however, the strategy employs modification of aptamers with PEG. We propose a one-step, simple strategy to deposit PEG by using an organic conducting polymers such as PPy as a foundation surface.

PPy has attracted considerable attention in the past decades to those developing biosensors because of its redox properties[16] and high electrical conductivity[17] along with it being a suitable interface for bio-receptor association.[18] It comes with several added advantages including the simplicity of polymerization and the high reproducibility of the resulting films. PPy has been used to immobilize various types of biomolecules by *e.g.* adsorption[19], entrapment during polymerization[20] and covalent linkage.[21] However, for covalent association, pyrrole monomers need prior chemical modification on their nitrogen or 3-substituted carbon positions to react with functional chemical groups such as carboxylic acids or amines.[22] Such an approach has been demonstrated with DNA sensors[23] and immunosensors.[24] However, the chemical modification of the pyrrole monomer can be time consuming. Miodek *et al.*[25] developed a faster method of functionalization of carbon nanotubes (CNTs) coated with un-modified PPy using macromolecular dendrimers PAMAM of forth generation. The electro-oxidation of the amine groups of dendrimers allow binding to both the CNTs and the PPy and allows further covalent attachment of biomolecules.

In this work, we design an aptasensor specific for human recombinant AMACR 1A protein based on PEG electro-patterned onto a PPy layer and associated with an ANTA/Cu^{2+} complex. Modification of a PPy film by PEG molecules can lead to minimization of non-specific binding. On the other hand, the association of redox molecules such as copper complexes with PPy can enhance the electrical properties of the film and improve the sensitivity of detection.[26] Electrochemical patterning was possible by functionalization of PEG on one terminus with amine groups that allow linking to PPy *via* radical cations formed during electro-oxidation. The second edge of the PEG's chains were modified with carboxylic acids, which allow further association of molecules. Poly-histidine modified DNA aptamers specific to AMACR were immobilized onto the PPy-PEG backbone through the ANTA/Cu^{2+} complex. This complex was covalently linked to the free carboxylate end of the PEG chain using EDC/NHS coupling agents.

The resultant biosensor was used for sensitive detection of AMACR in both buffer and spiked human plasma samples. The interaction of the target with the aptamer was detected by measuring variations in the electrochemical signal of copper. A sensitivity down to 5 fM was obtained using the

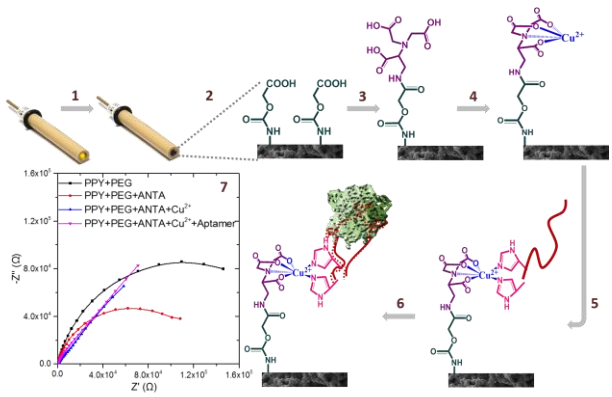

Figure 1: Schematic representation of aptasensor manufacture: (1) Electro-deposition of pyrrole on gold electrodes; (2) subsequent electro-patterning of PEG molecules using the amine present on one of its terminus; (3) Attachment of ANTA to the carboxyl end of PEG via covalent bonding with EDC/NHS coupling agents; (4) Immobilization of copper ions; (5) Immobilization of His-tagged DNA aptamers; (6) detection of AMACR; (7) Electrochemical impedance spectroscopy characterization of different layers.

square wave voltammetry (SWV) technique. The biosensor was characterized using scanning electron microscopy (SEM), Fourier-transform infrared spectroscopy (FTIR), electrochemical impedance spectroscopy (EIS) and cyclic voltammetry (CV). We also present a Surface Plasmon Resonance (SPR) study to demonstrate the proof of concept. The strategy presented can be generalized to other biosensors using different probes specific for the target analyte.

RESULTS AND DISCUSSION

Characterization of electro-generated PPy-PEG material

Figure 1 presents a schematic of the fabrication strategy (1-6) and a series of impedance spectrum illustrating changes in conductivity of the electrode during the formation of the different layers (7). The optimal conditions of polymerization and PEG association were obtained by investigating different parameters such as thickness of PPy layer and potential range for electro-deposition (see also Figures S2 to S4 in Supporting Information). Briefly, a clean gold electrode surface was modified with PPy by scanning the potential from -0.4 V to 0.9 V *vs.* Ag/AgCl with a scan rate of 100 mV.s^{-1} in the presence of 50 mM pyrrole monomer dissolved in H_2O containing 0.5 M lithium perchlorate for two cycles. From the EIS data, a small charge transfer resistance (R_{ct}) of 40 Ω was observed (see Figure S5 in Supporting Information). The film obtained showed a characteristic 'sickle shaped' morphology distributed across the electrode surface when observed under a scanning electron microscope (see Figure S1a in Supporting Information). This shape is characteristic of PPy when polymerization occurs in aqueous solutions.[27]

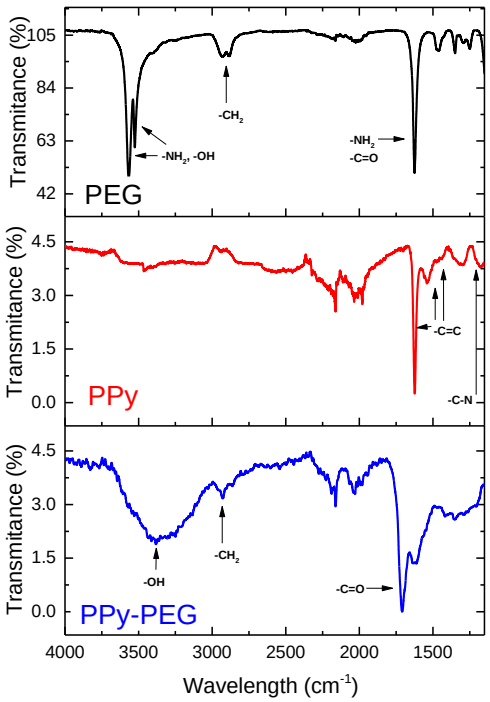

Figure 2: FTIR analysis of PEG adsorbed on gold chip and PPy layer before and after modification with PEG.

In order to modify the generated PPy film with PEG bearing both amine and carboxylic groups, electrochemical grafting of PEG was performed using the optimized conditions (see Figure S2 in Supporting Information). The modification was realized by the electrochemical oxidation of amine groups of PEG by scanning the potential between 0 V and 1.1 V *vs.* Ag/AgCl for 5 cycles during which PEG was covalently anchored onto the PPy layer. The mechanism of such a reaction assumes formation of radical cations on nitrogen atoms, which covalently attach to nucleophilic groups such as aromatic rings resulting in the rupture of the double carbon=carbon bond and formation of carbon-nitrogen bonds.[28]

From Figure 1.7 it can be seen that a high R_{ct} of *ca.* 200 kΩ was obtained after electrochemical PEG deposition. For comparison, electrodes immersed in PEG solution with no electrochemical oxidation showed an insignificant change in impedance (see Figure S5 in Supporting Information); this further validates the electrodeposition approach. Such electrochemical functionalization has been demonstrated earlier in the case of attachment of aliphatic amines to surfaces such as glassy carbon[29] or carbon nanotubes[28b] and recently on carbon nanotubes coated with PPy material.[25]

The electrochemical grafting of PEG on PPy film was further characterized with FTIR for PEG adsorbed on the gold surface, PPy film, and finally modified PPy with PEG (Figure 2). From the FTIR spectrum of PEG, one can see characteristic peaks of primary amine bonds at 3566 cm^{-1} and 1623 cm^{-1}, which can be also assigned to the –OH and C=O groups. For unmodified PPy, peaks at 1623 cm^{-1}, 1539 cm^{-1} and 1441 cm^{-1}, corresponding to C-N and C=C vibrations, were observed. Modification of PPy by PEG led to appearance of -OH and -C=O vibrations at 3364 cm^{-1} and 1709 cm^{-1}, respectively, confirming the presence of carboxylate groups on the surface and modification of polymer. The presence of the PEG's alkyl

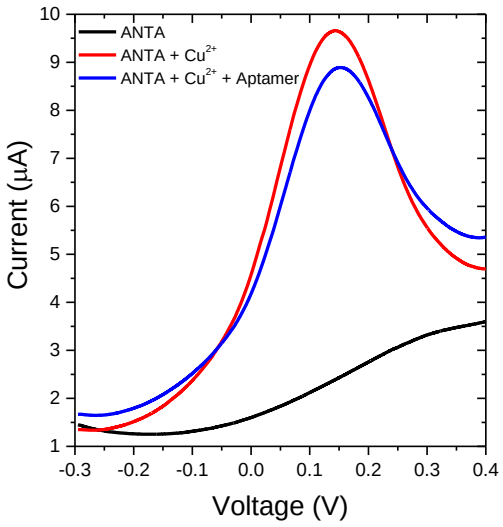

Figure 3: SWV characterization of copper ions immobilization followed by immobilization of DNA aptamers measured in PBS pH 7.4 V vs. Ag/AgCl.

chain is confirmed by the peak at 2934 cm^{-1}. Also a decrease in intensity of the C=C bond stretching was observed, which could be attributed to the attachment of PEG to double bonds present in the PPy structure, and confirming the mechanism of the reaction.

Association of biomolecules

In order to increase sensitivity of the biosensor, the PPy-PEG material was associated with an ANTA/Cu^{2+} complex as a redox marker. The formation of such a complex has been widely studied and is known to be very stable.[30] First, ANTA was linked by its amine group to the activated carboxylic acid present on the free end of PEG, using EDC/NHS chemistry. This was followed by saturation of the surface with ethanolamine. Modification with ANTA caused a decrease in impedance of the layer and also a decrease in capacitance. Such a decrease can be attributed to stabilization and reorganization of the grafted PEG polymer. This was confirmed using cyclic voltammetry (CV) in the presence of a ferro/ferricyanide $[Fe(CN)_6]^{3-/4-}$ redox couple, where an increase in redox signal was observed after binding of ANTA to the PEG surface (see Figure S6 and S7 in Supporting Information).

The complex between ANTA and a copper ion was formed by interaction of the metal in sodium acetate buffer, according to the procedure described by Chebil *et al.*[26a] The time used and the concentration of copper ions were crucial for this process and these were thoroughly optimized (see Supporting Information). Finally, histidine-tagged aptamers were immobilized on the surface by coordination of copper with two N-imidazole rings of the modified aptamers. During this process, bivalent metal ions such as Cu^{2+} bound to ANTA anchored on the surface by a tetravalent chelation, leaving two available coordination sites for the histidine modified aptamers. ANTA/Cu^{2+} form a stable complex and the binding of Cu^{2+} to the ANTA-modified self-assembled monolayer was studied by Stora *et al.*, showing a dissociation constant of 5 nM obtained with impedimetric measurements[31].

The formation of the biolayer was monitored using square wave voltammetry (SWV). Figure 3 shows a characteristic oxidation peak of copper at 0.15 V *vs.* Ag/AgCl after attachment on ANTA. This peak can be attributed to the Cu^{2+}/Cu^{+} reaction that occurs on the electrode surface. Copper peaks were also investigated by incubating the electrode at different steps of the layer formation, results from which are presented in the Supporting Information. The charge exchanged during the redox process allows calculation of the surface coverage of immobilized copper ions, following the equation:

$$\Gamma = Q/nFA \qquad (1)$$

Where Q is the charge under the cathodic or anodic peaks, n is number of electrons involved in the redox process, F is the Faraday constant, and A is the area of the electrode. Based on equation (1) we calculated the average coverage of the surface as 3.9 ± 0.4 pmol.cm^{-2}.

A reduction in the current corresponding to this peak was observed after attachment of His-tagged DNA aptamers. This could be related to a lower electron transfer or slower diffusion of electrolyte to the surface during the redox process due to the attachment of large molecules such as DNA. Such behavior was previously observed when PPy was associated with redox markers such as ferrocene[25] or copper complex.[26b] The biolayer formation was confirmed by SPR (see Supporting Information).

Anti-fouling properties of PPy-PEG-ANTA/Cu^{2+} complex

In order to evaluate the selectivity performance of the manufactured sensor, it was important to test its cross reactivity and nonspecific binding with other prostate cancer biomarkers. The fabricated aptasensor showed a significant variation of oxidation current peak of Cu^{2+} when it was incubated with 10 nM AMACR in 10 mM PBS pH 7.4. The DNA aptamer being specific to AMACR meant that the sensor showed a decrease in copper peak signal of 37% of relative current changes measured at 0.15 V *vs.* Ag/AgCl (Figure 3). This decrease is due to the blocking effect of electron transfer after attachment of proteins.[26] The sensor was then tested with other biomarkers for PCA such as 10 nM prostate specific antigen (PSA), 10 nM PSA-α1-antichymotrypsin (PSA-ACT) and 10 nM human kallikrein 2 (hK2). The aptasensor showed an efficient selective performance where the signal change was less than 3% in the presence of these other proteins, when compared to PBS alone.

To demonstrate an improved anti-fouling chemistry, the aptasensor was tested with human serum albumin (HSA), which is the most abundant protein present in blood. For the same, the electrodes were dipped in a solution containing 4% w/v HSA in buffer and the biosensor response was recorded. The aptasensor demonstrated an excellent anti-fouling efficiency with a signal change of less than 4% (see Figure 4 inset).

In order to underline the anti-fouling effect of the PEG surface, we investigated another molecule such as β-alanine ($H_2NCH_2CH_2COOH$) in *lieu* of PEG. β-Alanine was deposited onto the PPy layer in the same way that PEG was deposited and an aptasensor was manufactured. This β-alanine-based aptasensor was incubated with 4% (w/v) HSA in buffer and the electrochemical signal change was monitored as before. From the Figure 4 inset, it can be seen a significant relative current variation of up to 25%, demonstrating a poor anti-

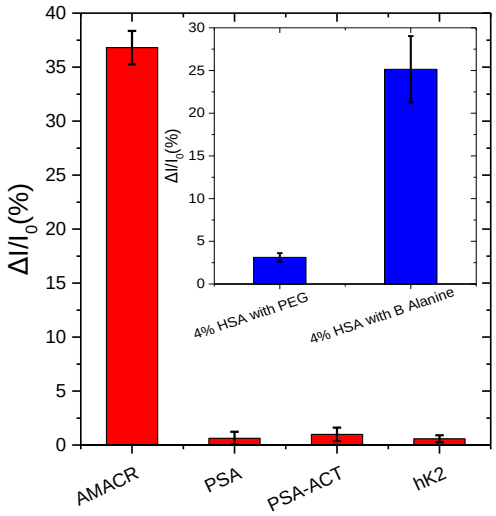

Figure 4: Selectivity study with other biomarkers for prostate cancer. Inset depicting the efficacy of PEG surface over β-alanine surface. Relative current changes $\Delta I/I_0$, where $\Delta I=(I_0-I)$, where I_0 is the peak current prior addition of the DNA target and I after incubation of the sensor with certain concentration of target. Data are means from 4 independent electrodes ± standard deviation.

fouling efficiency for this aptasensor. These results confirm that it is the presence of PEG that gives the sensor good anti-fouling properties.

Analytical performance of the biosensor

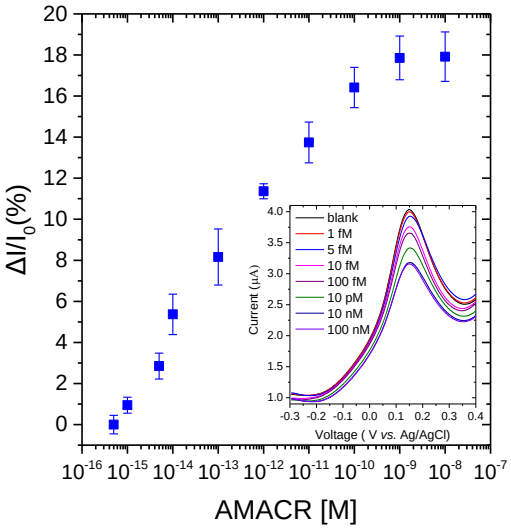

Figure 5. Calibration curve in AMACR spiked human plasma samples using SWV delta current. The plot of the relative changes of the current peak vs. concentration of DNA target measured at 0.15 V. Relative current changes $\Delta I/I_0$, where $\Delta I=(I_0-I)$, where I_0 is the peak current prior addition of the AMACR target and I after incubation of the sensor with certain concentration of target. Inset shows the real time SWV graphs obtained with different concentrations of AMACR. Data are means from 4 independent electrodes ± standard deviation.

The formation of the biolayer as well as detection of target were also successfully monitored using SWV by measuring the Cu^{2+}/Cu^{+} redox signal variation at 0.15 V *vs.* Ag/AgCl. The aptasensor demonstrated good reproducibility, which was characterized by monitoring the initial copper peaks obtained from each sample. A mean current peak of 4.27 ± 0.26 μA was obtained using 4 independent samples. The PEG aptasensor was initially tested with a wide range of AMACR concentrations from 1 fM to 10 nM in 10 mM PBS pH 7.4, where a decrease in redox signal was observed upon increasing AMACR concentration. The aptasensor demonstrated a sensitive response (Figure S9 in Supporting Information). The sensor could discriminate AMACR concentrations down to 5 fM. A limit of detection (LOD) of 0.15 fM was calculated using 5 independent samples as explained by Armbruster *et al*.[32] The system was further validated using surface plasmon resonance(SPR) technique, where the chip was fabricated with s similar surface chemistry and a dose response curve was obtained with detection down to 1 nM (see Figure S10c).

The aptasensor was further tested with human plasma samples. The electrodes were initially stabilized in human plasma without AMACR protein. Upon stabilization, spiked human plasma samples supplemented with AMACR were tested. The recorded signal after stabilization was used as a reference to calculate relative changes of current during detection of protein. Again a wide range of AMACR concentrations was tested from 1 fM to 10 nM.

The dose response curve is shown in Figure 5. A reduction in signal change was observed when compared with measurements in buffer, which can be attributed to the blocking effect by the histidine residues present in human plasma proteins.[33] From Figure 5, a redox signal variation of 2.85 $\pm$ 0.39% was obtained for 5 fM of AMACR concentration with a saturation at 10 nM corresponding to signal changes of 17.92 $\pm$ 1.2%. The electrochemical signal variations expressed in percentage were also compared with the absolute signal change (ΔI). The absolute signal change (ΔI) was obtained for each sample and a calibration curve was obtained using different concentrations of AMACR (Figure S13 in Supplementary Information). A current decrease of 0.14 $\pm$ 0.05 μA was obtained with 5 fM of AMACR and a maximum response was obtained with 10 nM of AMACR concentration with a variation of 0.84 $\pm$ 0.09 μA. Nevertheless, the sensor demonstrated a good response down to concentrations of 5 fM with a LOD of 1.4 fM. The dose response curve exhibits a linear response between 1fM and 1 nM. The inset of Figure 5 shows the SWV curves obtained with different concentrations of AMACR in human plasma. The sensor starts saturating at around 10 nM. These measurements were highly reproducible with relative standard deviations of 0.3-1.2% for 5 independent repeats. The efficiency of the sensor could be further improved by replacing copper ions with ferrocene as demonstrated in literature.[25]

CONCLUSIONS

We present a simple method of manufacturing a highly sensitive electrochemical aptasensor for detection of AMACR. We demonstrate that by electro-engineering PEG on the surface of a PPy film, anti-fouling properties can be significantly enhanced without loss of sensitivity. The modified PPy film with PEG-NTA/Cu^{2+}-Aptamer was successfully used to detect AMACR both in spiked buffer and human plasma samples. A low sensitivity value of 5 fM was attained with a LOD of 0.15 fM in buffer and 1.4 fM in human plasma, respectively. The sensor also demonstrated good selectivity when challenged with other prostate cancer biomarkers. This surface chemistry approach can be extended to the detection of a wide range of biomarkers by using suitable aptamers.

EXPERIMENTAL SECTION

Materials and Reagents

Histidine tagged AMACR-specific DNA aptamers [5'$(His)_6$TTTTTTCCCTACGGCGCTAACCCATGCTACGAATTCGTTGTTAAACAATAGGCCACCGTGCTACAA-3'], were obtained from Eurogentec, U.K. Prostate specific antigen (PSA) from human semen was obtained from Fitzgerald (U.S.A.). Human glandular kallikrein 2 (hK2) was obtained from R&D Systems, U.K. Complexed prostate specific antigen (PSA-ACT) was obtained from Lee Biosolutions, U.S.A. Phosphate buffered saline (PBS) tablets, pyrrole, ethanolamine, human serum albumin (HSA), lithium perchlorate, copper acetate, Nα,Nα-Bis(carboxymethyl)-L-lysine hydrate (ANTA), sodium acetate, poly(ethylene glycol) 2-aminoethyl ether acetic acid (PEG), potassium hexacyanoferrate (III), potassium hexacyanoferrate(II) trihydrate, N-hydroxysuccinimide (NHS), N-(3-dimethylaminopropyl)-N′-ethylcarbodiimidehydrochloride (EDC) were all purchased from the Sigma-Aldrich Chemical Co., U.K. All reagents were of analytical grade and were used without further purification. All aqueous solutions were prepared using 18.2 $M\Omega.cm^{-1}$ ultra-pure water from a Milli-Q system (Millipore, MA, U.S.A.). Human recombinant AMACR 1A was expressed from the plasmid reported by Darley *et al*.[34] and purified as described by Yevglevskis *et al*.[35]

Apparatus

The electrochemical measurements were performed using a μAUTOLAB III / FRA2 potentiostat (MetrohmAutolab, The Netherlands) using a three-electrode cell setup with a Ag/AgCl reference electrode (BASi, U.S.A.) and a Pt counter electrode (ALS, Japan). The impedance spectrum was measured in 10 mM PBS measurement buffer (pH 7.4) with a 10 mV a.c. voltage superimposed on a bias d.c. voltage of 0.17 V *vs*. Ag/AgCl. Cyclic voltammetry was performed in 10 mM PBS (pH 7.4) in the range from -0.2 V to 0.35 V without redox couple and -0.4 V to 0.45 V in 10 mM PBS containing 10 mM ferro/ferricyanide $[Fe(CN)_6]^{3-/4-}$. Square wave voltammetry was performed in 10 mM PBS (pH 7.4) in the potential range from -0.3 V to 0.4 V with a conditioning time of 120 s, modulation amplitude of 20 mV and frequency of 50 Hz.

Gold disk working electrodes with a radius of 1.0 mm (CH Instruments, U.S.A.) were first cleaned by mechanical polishing for 5 min with 50 nm alumina slurry (Buehler, U.K.) on a polishing pad (Buehler, U.K.) followed by 5 min sonication in ethanol and then in water. The electrodes were then subjected to chemical cleaning with piranha solution (3 parts of concentrated H_2SO_4 with 1 part of H_2O_2 for 5 min). The electrodes were then rinsed with Milli-Q water. Thereafter, electrodes were electrochemically cleaned in 0.5 M H_2SO_4 by scanning the potential between the oxidation and reduction of gold, –0.05 V and +1.1 V versus an Hg/Hg_2SO_4 reference electrode, for 50 cycles until no further changes in the volt-

ammogram were observed. Finally, electrodes were washed with Milli-Q water.

Fourier Transform Infrared spectra (FTIR) were measured using a Spectrum 100 FT-IR spectrometer (PerkinElmer, U.K.) equipped with an attenuated total reflectance (ATR) diamond crystal. For FTIR, SPR gold chips were used. Surface characterization of PPy coated gold SPR chips were performed using a scanning electron microscopy (JSM-6480Jeol, Japan) at 1000X magnification with acceleration voltage of 5 kV to acquire SEM images.

Surface plasmon resonance (SPR) measurements were performed using a Reichert SPR 7000DC (U.S.A.) dual channel flow at 25 °C. 50 nm gold coated SPR gold chips, supplied from Reichert Technologies were used for studying the reaction on SPR. Prior to their modification, chips were cleaned using piranha solution (3:1 H_2SO_4:H_2O_2) for 20 seconds and rinsed thoroughly with MilliQ water and dried using nitrogen gas. All buffers were filtered through 0.2 µm filters and degassed for 2 h by sonication prior to the experiment.

Electro-chemical deposition of PEG

The polypyrrole film (PPy) was grown on the gold surface by cycling the potential from -0.4 V to 0.9 V *vs.* Ag/AgCl, with a scan rate of 100 $mV.s^{-1}$ for 2 cycles in Milli-Q water containing 0.5 M $LiClO_4$. Electro-polymerization was performed using a three-electrode configuration in a small volume cell (BASi, USA) containing 250 µL of 50 mM pyrrole monomer. After reaction the electrode was rinsed with Milli-Q water.

PEG was immobilized on the PPy film by covalent bonding *via* electro-oxidation of the amine groups of PEG. The procedure was again performed in the small volume cell containing 250 µL of 1 mM PEG dissolved in Milli-Q water containing 0.5 M $LiClO_4$ by cycling the potential from 0.0 V to 1.1 V *vs*. Ag/AgCl during 5 cycles with a scan rate of 50 $mV.s^{-1}$.

Immobilization of ANTA/Cu^{2+} complex and His-tagged aptamers

Immobilization of ANTA/Cu^{2+} complex and the His-tagged aptamers was performed using the protocol reported by Chebil *et al*.[26a] The carboxylic acid groups on the free end of the deposited PEG was used to covalently attach N-(5-Amino-1-carboxypentyl)iminodiacetic acid (ANTA). First, electrodes were subjected to a 2:1 ratio of EDC/NHS (160 mM/80 mM) in water for 20 minutes. Electrodes were then rinsed with Milli-Q water and immersed in 7 mM ANTA dissolved in 10 mM PBS (pH 8.5) for 30 minutes. The electrodes were then rinsed with Milli-Q water and the unreacted activated carboxylate groups were blocked with 10 mM ethanolamine (pH 8.5) for 30 minutes. Finally the electrodes were immersed in a solution of 3.5 mM copper acetate dissolved in 20 mM acetate buffer (NaOAc/HCl, pH 4.6) for 25 minutes. During the process, the copper molecules associated with the ANTA attached to the surface *via* coordinate chemistry. Anti-AMACR aptamers (0.5 µM in 10 mM PBS, pH 7.4) were preheated at 95°C for 5 min and gradually cooled down to room temperature over 25 min.[9] Activated His-tagged anti-AMACR aptamers were immobilized to the copper complexes *via* coordination of two of the N-imidazole rings of the His-tag with copper.

Detection of AMACR

Detection of AMACR with DNA aptamers immobilized on the surface was achieved by incubating the aptasensor in the solution containing AMACR for 30 min at ambient room temperature. A wide range of AMACR concentrations were used: 1, 10, 100 fM; 1, 10, 100 pM; 1, 10 nM in 10 mM PBS buffer, pH 7.4 and 1 to 10 diluted human plasma (diluted in 10 mM PBS, pH 7.4) spiked samples. The concentration of AMACR stock solutions was determined by UV-visible spectroscopy.

ASSOCIATED CONTENT

Supporting Information

The Supporting Information is available free of charge on the ACS Publication website.

Detailed Aptasensor optimization steps, SEM micrograph of polypyrrole film and electrochemical characterization studies together with surface plasmon resonance studies for biosensor layer by layer fabrication and detection of AMACR is presented. It also presents the obtained dose response curve obtained in buffer solutions (pdf).

AUTHOR INFORMATION

Corresponding Author

* P.Estrela@bath.ac.uk; *Anna_Miodek@yahoo.com

Department of Electronic & Electrical Engineering,

University of Bath, Claverton Down, Bath, BA2 7AY, United Kingdom

Phone: +44-1225-386324

Notes

The authors declare no competing financial interest.

ACKNOWLEDGMENTS

This work was funded by the European Commission FP7 Programme through the Marie Curie Initial Training Network PROSENSE (grant no. 317420, 2012-2016). AM was funded by the Defence Science and Technology Laboratory through contract No. Dstlx-1000074164.

REFERENCES

1. Partin, A. W.; Kattan, M. W.; Subong, E. N.; Walsh, P. C.; Wojno, K. J.; Oesterling, J. E.; Scardino, P. T.; Pearson, J., Combination of prostate-specific antigen, clinical stage, and Gleason score to predict pathological stage of localized prostate cancer: a multi-institutional update. *JAMA - Journal of the American Medical Association* **1997,** *277* (18), 1445-1451.

2. Sreekumar, A.; Laxman, B.; Rhodes, D. R.; Bhagavathula, S.; Harwood, J.; Giacherio, D.; Ghosh, D.; Sanda, M. G.; Rubin, M. A.; Chinnaiyan, A. M., Humoral immune response to α-methylacyl-CoA racemase and prostate cancer. *Journal of the National Cancer Institute* **2004,** *96* (11), 834-843.

3. Jolly, P.; Formisano, N.; Estrela, P., DNA aptamer-based detection of prostate cancer. *Chemical Papers* **2015,** *69* (1), 77-89.

4. (a) Lloyd, M.D., Darley, D.J., Wierzbicki, A.S. and Threadgill, M.D., α-Methylacyl-CoA racemase–an 'obscure'metabolic enzyme takes centre stage. *FEBS Journal*, **2008**, 275(6), pp.1089-1102 (b) Li, C.F., Fang, F.M., Lan, J., Wang, J.W., Kung, H.J., Chen, L.T., Chen,

T.J., Li, S.H., Wang, Y.H., Tai, H.C. and Yu, S.C., AMACR amplification in myxofibrosarcomas: a mechanism of overexpression that promotes cell proliferation with therapeutic relevance. *Clinical Cancer Research*, **2014**, 20 (23), pp.6141-6152.

5. Jiang, Z.; Wu, C.; Woda, B.; Iczkowski, K.; Chu, P.; Tretiakova, M.; Young, R.; Weiss, L.; Blute, R.; Brendler, C., Alpha-methylacyl-CoA racemase: a multi-institutional study of a new prostate cancer marker. *Histopathology* **2004,** *45* (3), 218-225.

6. (a) Jiang, Z.; Woda, B. A.; Rock, K. L.; Xu, Y.; Savas, L.; Khan, A.; Pihan, G.; Cai, F.; Babcook, J. S.; Rathanaswami, P., P504S: a new molecular marker for the detection of prostate carcinoma. *American Journal of Surgical Pathology* **2001,** *25* (11), 1397-1404; (b) Zhou, M.; Chinnaiyan, A. M.; Kleer, C. G.; Lucas, P. C.; Rubin, M. A., Alpha-Methylacyl-CoA racemase: a novel tumor marker over-expressed in several human cancers and their precursor lesions. *American Journal of Surgical Pathology* **2002,** *26* (7), 926-931; (c) Rubin, M. A.; Zhou, M.; Dhanasekaran, S. M.; Varambally, S.; Barrette, T. R.; Sanda, M. G.; Pienta, K. J.; Ghosh, D.; Chinnaiyan, A. M., α-Methylacyl coenzyme A racemase as a tissue biomarker for prostate cancer. *JAMA - Journal of the American Medical Association* **2002,** *287* (13), 1662-1670; (d) Luo, J.; Zha, S.; Gage, W. R.; Dunn, T. A.; Hicks, J. L.; Bennett, C. J.; Ewing, C. M.; Platz, E. A.; Ferdinandusse, S.; Wanders, R. J., α-Methylacyl-CoA Racemase A New Molecular Marker for Prostate Cancer. *Cancer Research* **2002,** *62* (8), 2220-2226.

7. Rogers, C. G.; Yan, G.; Zha, S.; Gonzalgo, M. L.; Isaacs, W. B.; Luo, J.; De Marzo, A. M.; Nelson, W. G.; Pavlovich, C. P., Prostate cancer detection on urinalysis for α methylacyl coenzyme a racemase protein. *Journal of Urology* **2004,** *172* (4), 1501-1503.

8. (a) Maraldo, D.; Garcia, F. U.; Mutharasan, R., Method for quantification of a prostate cancer biomarker in urine without sample preparation. *Analytical Chemistry* **2007,** *79* (20), 7683-7690; (b) Lin, P.-Y.; Cheng, K.-L.; McGuffin-Cawley, J. D.; Shieu, F.-S.; Samia, A. C.; Gupta, S.; Cooney, M.; Thompson, C. L.; Liu, C. C., Detection of alpha-methylacyl-CoA racemase (AMACR), a biomarker of prostate cancer, in patient blood samples using a nanoparticle electrochemical biosensor. *Biosensors* **2012,** *2* (4), 377-387; (c) Wang, J.; Yau, S. T., Detection of α-Methylacyl-CoA Racemase in Serum and Urine Using a Highly Sensitive Electrochemical Immunodetector. *Electroanalysis* **2014,** *26* (7), 1441-1444.

9. Yang, D.-K.; Chen, L.-C.; Lee, M.-Y.; Hsu, C.-H.; Chen, C.-S., Selection of aptamers for fluorescent detection of alpha-methylacyl-CoA racemase by single-bead SELEX. *Biosensors and Bioelectronics* **2014,** *62*, 106-112.

10. McCauley, T. G.; Hamaguchi, N.; Stanton, M., Aptamer-based biosensor arrays for detection and quantification of biological macromolecules. *Analytical Biochemistry* **2003,** *319* (2), 244-250.

11. Nimjee, S. M.; Rusconi, C. P.; Sullenger, B. A., Aptamers: an emerging class of therapeutics. *Annual Review of Medicine* **2005,** *56*, 555-583.

12. (a) Sharma, S.; Johnson, R. W.; Desai, T. A., XPS and AFM analysis of antifouling PEG interfaces for microfabricated silicon biosensors. *Biosensors and Bioelectronics* **2004,** *20* (2), 227-239; (b) Statz, A. R.; Meagher, R. J.; Barron, A. E.; Messersmith, P. B., New peptidomimetic polymers for antifouling surfaces. *Journal of the American Chemical Society* **2005,** *127* (22), 7972-7973; (c) Rodriguez Emmenegger, C.; Brynda, E.; Riedel, T.; Sedlakova, Z.; Houska, M.; Alles, A. B., Interaction of blood plasma with antifouling surfaces. *Langmuir* **2009,** *25* (11), 6328-6333; (d) Nogues, C.; Leh, H.; Lautru, J.; Delelis, O.; Buckle, M., Efficient antifouling surface for quantitative surface plasmon resonance based biosensor analysis. *PLoS One* **2012**, 7 (9), e44287.

13. Estrela, P.; Paul, D.; Song, Q.; Stadler, L. K.; Wang, L.; Huq, E.; Davis, J. J.; Ferrigno, P. K.; Migliorato, P., Label-free sub-picomolar protein detection with field-effect transistors. *Analytical Chemistry* **2010,** *82* (9), 3531-3536.

14. Kjällman, T. H.; Peng, H.; Soeller, C.; Travas-Sejdic, J., Effect of probe density and hybridization temperature on the response of an electrochemical hairpin-DNA sensor. *Analytical Chemistry* **2008,** *80* (24), 9460-9466.

15. Hayat, A.; Andreescu, S.; Marty, J.-L., Design of PEG-aptamer two piece macromolecules as convenient and integrated sensing platform: Application to the label free detection of small size molecules. *Biosensors and Bioelectronics* **2013,** *45*, 168-173.

16. Han, D.-H.; Lee, H. J.; Park, S.-M., Electrochemistry of conductive polymers XXXV: Electrical and morphological characteristics of polypyrrole films prepared in aqueous media studied by current sensing atomic force microscopy. *Electrochimica Acta* **2005,** *50* (15), 3085-3092.

17. Andrade, J. D., Surface and interfacial aspects of biomedical polymers. Vol. 1. Surface chemistry and physics. *Plenum Press* **1985**, 470.

18. (a) Kausaite-Minkstimiene, A.; Mazeiko, V.; Ramanaviciene, A.; Ramanavicius, A., Evaluation of amperometric glucose biosensors based on glucose oxidase encapsulated within enzymatically synthesized polyaniline and polypyrrole. *Sensors and Actuators B* **2011,** *158* (1), 278-285; (b) Azioune, A.; Siroti, F.; Tanguy, J.; Jouini, M.; Chehimi, M. M.; Miksa, B.; Slomkowski, S., Interactions and conformational changes of human serum albumin at the surface of electrochemically synthesized thin polypyrrole films. *Electrochimica Acta* **2005,** *50* (7), 1661-1667; (c) Raoof, J.-B.; Ojani, R.; Rashid-Nadimi, S., Preparation of polypyrrole/ferrocyanide films modified carbon paste electrode and its application on the electrocatalytic determination of ascorbic acid. *Electrochimica Acta* **2004,** *49* (2), 271-280.

19. (a) Apetrei, C.; Rodríguez-Méndez, M.; De Saja, J., Amperometric tyrosinase based biosensor using an electropolymerized phosphate-doped polypyrrole film as an immobilization support. Application for detection of phenolic compounds. *Electrochimica Acta* **2011,** *56* (24), 8919-8925; (b) Ahuja, T.; Mir, I. A.; Kumar, D., Potentiometric urea biosensor based on BSA embedded surface modified polypyrrole film. *Sensors and Actuators B* **2008,** *134* (1), 140-145.

20. Wang, J.; Jiang, M.; Fortes, A.; Mukherjee, B., New label-free DNA recognition based on doping nucleic-acid probes within conducting polymer films. *Analytica Chimica Acta* **1999,** *402* (1), 7-12.

21. Cosnier, S., Biomolecule immobilization on electrode surfaces by entrapment or attachment to electrochemically polymerized films. A review. *Biosensors and Bioelectronics* **1999,** *14* (5), 443-456.

22. (a) Dong, H.; Cao, X.; Li, C. M.; Hu, W., An *in situ* electrochemical surface plasmon resonance immunosensor with polypyrrole propylic acid film: Comparison between SPR and electrochemical responses from polymer formation to protein immunosensing. *Biosensors and Bioelectronics* **2008,** *23* (7), 1055-1062; (b) Bisht, V.; Takashima, W.; Kaneto, K., A novel thin film urea biosensor based on copolymer poly (N-3-aminopropylpyrrole-co-pyrrole) film. *Surface and Coatings Technology* **2005,** *198* (1), 231-236; (c) Ionescu, R. E.; Jaffrezic-Renault, N.; Bouffier, L.; Gondran, C.; Cosnier, S.; Pinacho, D. G.; Marco, M.-P.; Sánchez-Baeza, F. J.; Healy, T.; Martelet, C., Impedimetric immunosensor for the specific label free detection of ciprofloxacin antibiotic. *Biosensors and Bioelectronics* **2007,** *23* (4), 549-555.

23. (a) Korri-Youssoufi, H.; Garnier, F.; Srivastava, P.; Godillot, P.; Yassar, A., Toward bioelectronics: specific DNA recognition based on an oligonucleotide-functionalized polypyrrole. *Journal of the American Chemical Society* **1997,** *119* (31), 7388-7389; (b) Peng, H.; Soeller, C.; Travas-Sejdic, J., Novel conducting polymers for DNA sensing. *Macromolecules* **2007,** *40* (4), 909-914.

24. Hafaid, I.; Chebil, S.; Korri-Youssoufi, H.; Bessueille, F.; Errachid, A.; Sassi, Z.; Ali, Z.; Abdelghani, A.; Jaffrezic-Renault, N., Effect of electrical conditions on an impedimetric immunosensor based on a modified conducting polypyrrole. *Sensors and Actuators B* **2010,** *144* (1), 323-331.

25. Miodek, A.; Mejri, N.; Gomgnimbou, M.; Sola, C.; Korri-Youssoufi, H., E-DNA Sensor of *Mycobacterium tuberculosis* Based on Electrochemical Assembly of Nanomaterials (MWCNTs/PPy/PAMAM). *Analytical Chemistry* **2015,** *87* (18), 9257-9264.

26. (a) Chebil, S.; Hafaiedh, I.; Sauriat-Dorizon, H.; Jaffrezic-Renault, N.; Errachid, A.; Ali, Z.; Korri-Youssoufi, H., Electrochemical detection of d-dimer as deep vein thrombosis marker using single-chain d-dimer antibody immobilized on functionalized polypyrrole. *Biosensors and Bioelectronics* **2010,** *26* (2), 736-742; (b) Chebil, S.; Miodek, A.; Ambike, V.; Sauriat-Dorizon, H.; Policar, C.;

Korri-Youssoufi, H., Polypyrrole functionalized with new copper complex as platform for His-tag antibody immobilization and direct antigen detection. *Sensors and Actuators B* **2013,** *185*, 762-770.

27. Carquigny, S.; Segut, O.; Lakard, B.; Lallemand, F.; Fievet, P., Effect of electrolyte solvent on the morphology of polypyrrole films: application to the use of polypyrrole in pH sensors. *Synthetic Metals* **2008,** *158* (11), 453-461.

28. (a) Zhang, L.; Jiang, X.; Wang, E.; Dong, S., Attachment of gold nanoparticles to glassy carbon electrode and its application for the direct electrochemistry and electrocatalytic behavior of hemoglobin. *Biosensors and Bioelectronics* **2005,** *21* (2), 337-345; (b) Adenier, A.; Chehimi, M. M.; Gallardo, I.; Pinson, J.; Vila, N., Electrochemical oxidation of aliphatic amines and their attachment to carbon and metal surfaces. *Langmuir* **2004,** *20* (19), 8243-8253.

29. Ghanem, M. A.; Chrétien, J.-M.; Pinczewska, A.; Kilburn, J. D.; Bartlett, P. N., Covalent modification of glassy carbon surface with organic redox probes through diamine linkers using electrochemical and solid-phase synthesis methodologies. *Journal of Materials Chemistry* **2008,** *18* (41), 4917-4927.

30. Khan, F.; He, M.; Taussig, M. J., Double-hexahistidine tag with high-affinity binding for protein immobilization, purification, and detection on ni-nitrilotriacetic acid surfaces. *Analytical Chemistry* **2006,** *78* (9), 3072-3079.

31. Stora, T.; Hovius, R.; Dienes, Z.; Pachoud, M.; Vogel, H.; Metal ion trace detection by a chelator-modified gold electrode: A comparison of surface to bulk affinity. *Langmuir* **1997**, 13(20), 5211-5214.

32. Armbruster, D. A.; Pry, T., Limit of blank, limit of detection and limit of quantitation. *Clinical Biochemist Reviews* **2008,** *29* (Suppl 1), S49-52.

33. Jones, A. L.; Hulett, M. D.; Parish, C. R., Histidine-rich glycoprotein: A novel adaptor protein in plasma that modulates the immune, vascular and coagulation systems. *Immunology and Cell Biology* **2005,** *83* (2), 106-118.

34. Darley, D. J.; Butler, D. S.; Prideaux, S. J.; Thornton, T. W.; Wilson, A. D.; Woodman, T. J.; Threadgill, M. D.; Lloyd, M. D., Synthesis and use of isotope-labelled substrates for a mechanistic study on human α-methylacyl-CoA racemase 1A (AMACR; P504S). *Organic and Biomolecular Chemistry* **2009,** *7* (3), 543-552.

35. Yevglevskis, M.; Lee, G. L.; Sun, J.; Zhou, S.; Sun, X.; Kociok-Köhn, G.; James, T. D.; Woodman, T. J.; Lloyd, M. D., A study on the AMACR catalysed elimination reaction and its application to inhibitor testing. *Organic and Biomolecular Chemistry* **2016**, 14 v(2), pp.612-622.